Xiaoping Zhan, Yuxuan Xin, Kai Zhao, Shuai Wang, Jian Chen, Yuankui Zhang and Zhenmin Mao*

Synthesis, characterization and molecular dynamics simulation of the polyacrylates membranes

DOI 10.1515/epoly-2015-0211
Received September 2, 2015; accepted October 27, 2015; previously published online December 8, 2015

Abstract: The aims of this paper are to investigate the inherent relationship between the structures of the polyacrylates and release behaviors as drug carriers in the transdermal drug delivery systems. Three model polyacrylates compounds were synthesized by radical polymerization. Three polymer materials were characterized by Fourier transform infrared, differential scanning calorimeter and cytotoxicity, and the release behaviors of drug molecules transporting through the polymers membranes were tested. Moreover, the effects of the polymers' structures on the permeability were studied by molecular dynamic simulation. The simulation results showed that higher chains mobility and larger fractional free volume of the polymer membranes resulted in higher permeation rates. By comparing the monomers' structure in the polymer materials, it was found that the polymer chains' mobility decreases, and permeation rate correspondingly decreases with the increase in the amount and volume of side groups on the double bonds.

Keywords: drug delivery system; molecular dynamics simulation; permeability; polyacrylates; rate-controlling membrane.

1 Introduction

The rate-controlling membrane is an important part in the transdermal drug delivery systems (TDDs) because it ensures the drug delivers at a predetermined rate. At present, rate-controlling membranes as drug-carrier materials used include chitosan (1–4), alginate (5), poly(lactic-co-glycolic acid) (6, 7), polyacrylic acid (8), polyethylene (9, 10), ethylene vinyl acetate (11, 12), nylon (13, 14), rubber (15, 16) and polyacrylate (17, 18). Among these drug-carrying materials, the polyacrylates are an important type owing to their perfect controlling-release properties and accessible radical polymerization reactions.

Free radical polymerization is a facile method for producing acrylate polymers, especially as the photopolymerization normally takes place within a range of seconds (19). The number of polyacrylates have a rapid increase owing to various monomer types. Moreover, acrylates polymers exhibit little toxicity although the monomers may be toxic (20). At present, these polyacrylates have been widely used in the fields of binders, film formers, suspending agents, viscosity-increasing agents, emulsion stabilizers, dental restorative materials and biomaterials (21).

In recent years, the gel-like polyacrylates have been used in the drug diffusion system. For example, poly(2-hydroxyethylmethacrylate), poly(2-hydroxyethylacrylate) and poly(alkyleneglycol) (meth)acrylates, are favorable as components of "smart" materials owing to their excellent biocompatibility and physicochemical properties (22–24).

In our previous work, a serial of film-like polyacrylates as the rate-controlling membranes in TDDs were described (17, 18, 25, 26). When drug molecules are transporting through these polyacrylates membranes, the drug molecules show different release behaviors. For example, when clonidine hydrochloride molecules in the aqueous solution transport through the membrane **1** (25), which is composed of 2-hydroxy-3-phenoxypropylacrylate (A), 4-hydroxybutyl acrylate (B) and dibutyl maleate (C1) monomer units with the weight fraction 4:4:2, the permeation rate is lower than that of the membrane **2** (26), which is composed of A, B and diethyl maleate (C2) monomer units with the weight fraction 4:4:2. Compared with their monomer units, it is found that the side groups on the double bonds in the monomer C1 and C2 are different. Thus, we know the side groups on the polymer main chains will have an impact on the drug release in the membrane.

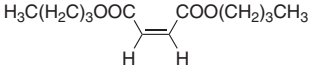

C1

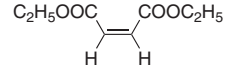

C2

***Corresponding author: Dr. Zhenmin Mao,** School of Pharmacy, Shanghai Jiaotong University, Shanghai 200240, China, e-mail: zmmao@sjtu.edu.cn
Xiaoping Zhan, Yuxuan Xin, Kai Zhao, Shuai Wang, Jian Chen and Yuankui Zhang: School of Pharmacy, Shanghai Jiaotong University, Shanghai 200240, China

However, until now, we cannot explain how the monomer's structure affects the release behavior of the drug molecules at a molecular level, because the release of the drug molecules inside the polymer membrane is an extremely complicated process. It is well known that the penetrant diffusion in the membrane is strongly dependent on free volume in the membrane and chain mobility of the polymer itself (27–31). We think a study on the relationship of structure and performance is necessary. If an inherent structure-performance relationship is explored, we can design polymers and predict its performance.

In this work, we choose a previously described membrane **3** of which monomer units were monomer A, monomer B and 2-butoxyethyl methacrylate (C3) with the weight fraction of 4:4:2 as a referencing polymer (17). On the basis of the monomer units of membrane **3**, monomer C3 is replaced with monomers C4, C5 and C6, respectively, the corresponding polymers **4**, **5** and **6** are synthesized by the reaction of radical polymerization. Monomer C4 is less a substituted methyl group on the C=C bond than monomer C3, monomer C5 is 2-butoxyethyl of monomer C3 replaced with 2-phenoxy ethyl, monomer C6 is 2-butoxyethyl of monomer C3 replaced with isodecyl.

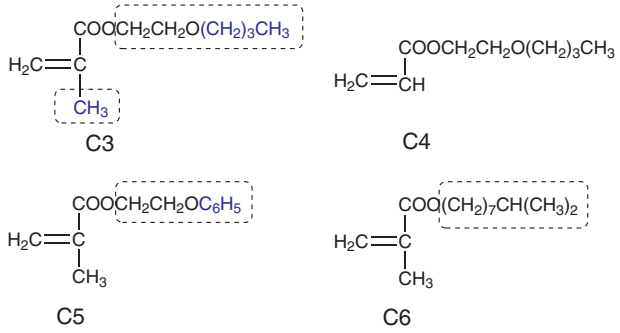

In order to explore the relationship between the structure of the polyacrylates and release behaviors, the model's polymer compounds were characterized by a differential scanning calorimeter, the release behavior was tested by the *in vitro* release experiment, and the fractional free volume of the polymer membrane and the mobility of the polymer chains were investigated by a molecular dynamics simulation.

2 Results and discussion

2.1 Characterization of the polyacrylates membrane

The Fourier transform infrared (FTIR) spectra of the membranes **4**, **5** and **6** are recorded in Figure 1. The three membranes have similar characteristic peaks in the FTIR spectra owing to 80% of A and B in the monomer units. Here the characteristic peaks of the membrane **4** are assigned in detail: a wide peak from 3600 to 3200 cm^{-1} is the stretching vibration of O-H, 2954 cm^{-1} is the stretching vibration of C-H; 1598, 1494 and 1454 cm^{-1} are the aromatic ring skeleton vibration; 758 and 694 cm^{-1} are the bending vibration of C-H in the aromatic ring; 1732 cm^{-1} is the stretching vibration of C=O in ester group; 1174 cm^{-1} is the stretching vibration of C-O-C in ester group; 1245 cm^{-1} is the stretching vibration of C-O in O-C_6H_5; 1045 cm^{-1} is the stretching vibration of C-O in CH_2OH. The absence of absorption peaks at ~1620 cm^{-1} and ~810 cm^{-1} implies the successful reaction of radical polymerization with the C=C bonds in the monomer units (32, 33).

The assignment of absorption peaks in the FTIR spectra of membrane **5** are 3600–3200 cm^{-1} (ν_{O-H}), 2952 cm^{-1} (ν_{C-H}), 1598, 1496 and 1456 cm^{-1} (ν_{C-C}, aromatic ring), 752 and 692 cm^{-1} (δ_{C-H}, aromatic ring), 1732 cm^{-1} ($\nu_{C=O}$), 1172 and 1244 cm^{-1} (ν_{C-O-C}), 1045 cm^{-1}($\nu_{C-O(H)}$). The assignment of absorption peaks in the FTIR spectra of the membrane **6** are 3600–3200 cm^{-1} (ν_{O-H}), 2956 cm^{-1} (ν_{C-H}), 1598, 1496 and 1456 cm^{-1} (ν_{C-C}, aromatic ring), 756 and 692 cm^{-1} (δ_{C-H}, aromatic ring), 1733 cm^{-1} ($\nu_{C=O}$), 1172 and 1247 cm^{-1} (ν_{C-O-C}), 1045 cm^{-1} ($\nu_{C-O(H)}$).

The differential scanning calorimetry (DSC) thermograms of membranes **4**, **5** and **6** are recorded in Figure 2. The values of the T_g of the membranes **4**, **5** and **6** were -10.776, 20.354 and 8.148°C, respectively.

2.2 *In vitro* cytotoxicity studies

Cytotoxicity is one of the important properties for biomedical material. The 3-(4,5-dimethylthiazol-2-yl)-2,5-diphenyltetrazoliumbromide (MTT) assay is widely used to evaluate the *in vitro* cytotoxicity. It is based on the reaction between MTT and mitochondrial succinate dehydrogenases in living cells to form a purple formazan which is not soluble in water but is soluble in dimethyl sulfoxide (DMSO). Cytotoxicity of the liquid extracts of the polyacrylates membrane was tested by the MTT assay in L929 cells.

Usually, the cytotoxic effects in cell cultures are mainly caused by released monomers. When the curing of a polyacrylate is not complete, unconverted monomers can be released from the polymer into the medium phase and cause cytotoxicity. Table 1 shows the relative growth ratio (RGR) data of the membranes **4**, **5** and **6**. During the 3-day cell culture period, all the RGR values were above 90%. This indicated that all polymers presented very low cytotoxicity.

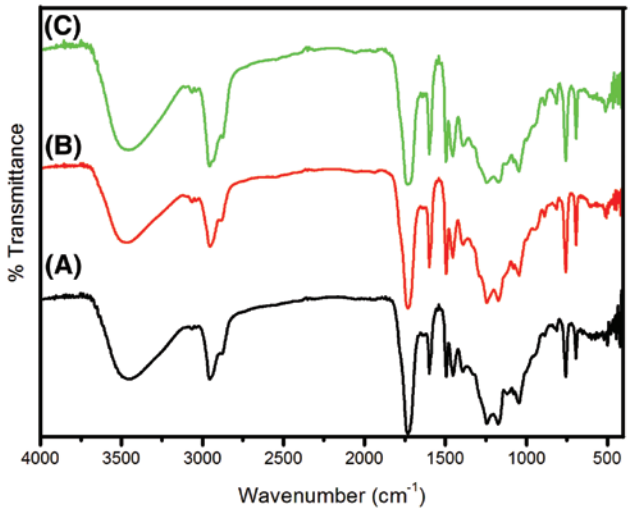

Figure 1: The FTIR spectra of the membranes: (A) membrane **4**, (B) membrane **5** and (C) membrane **6**.

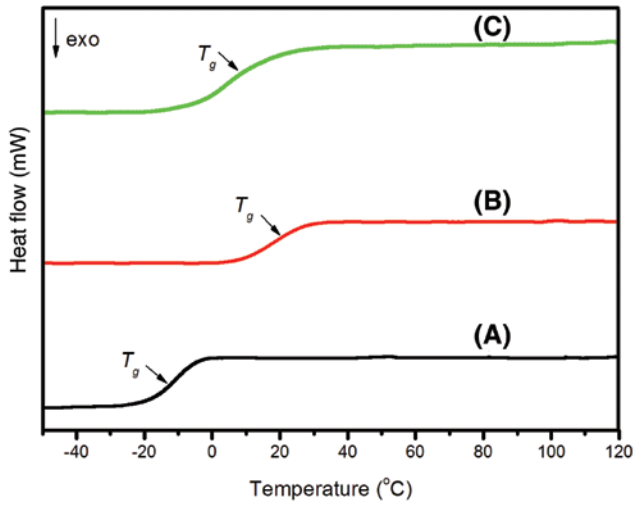

Figure 2: The DSC thermograms of the membranes: (A) membrane **4**, (B) membrane **5** and (C) membrane **6**.

Table 1: RGR values of the membranes after 1, 2 and 3-day's culture (mean±SD n=3).

Membrane	RGR (%)		
	1 day	2 day	3 day
4	93.03±6.84	90.10±5.89	90.01±3.17
5	98.13±4.40	90.02±3.12	94.17±2.21
6	97.63±5.66	92.13±5.50	93.64±5.18

2.3 *In vitro* release of clonidine HCl

Table 2 depicts the cumulative amount of clonidine transporting through the membranes **4**, **5** and **6** with 14 μm thickness. Compared with the previous reported membrane **3** (17), the permeation rates follow the order of membrane **4**>membrane **3**>membrane **6**>membrane **5**.

2.4 Effect of the structure of the polymers on the release behaviors

It is well known that the release molecules firstly are absorbed onto the membrane and then diffuse through it. Usually, the release rate of drug molecules in the membrane is considerably affected by the mobility of polymer chains (29, 31) and free volume of the polymer membrane (27, 28).

The mobility of polymer chains can be analyzed by the MSD of the polymer chains. The larger slope of the MSD curve reflects the higher chains' mobility. The MSD of the polymer chains are shown in Figure 3. It was found that the chains' mobility follows the order of membrane **4**>membrane **3**>membrane **6**>membrane **5**. As we know the glass transition temperature (T_g) is another parameter to reflect the mobility of polymer chains by experimental measurement. Lower T_g value reflects the higher chains'

Table 2: The permeation rates of the membranes (mean±SD n=3).

Membrane	*J* [μg/(cm²·h)]	Correlation coefficient (*r*)
3[a]	34.388±0.426 (17)	0.9985 (17)
4	35.067±0.841	0.9971
5	12.483±0.372	0.9976
6	29.762±0.479	0.9994

[a]The values of *J* and *r* were taken from (17).

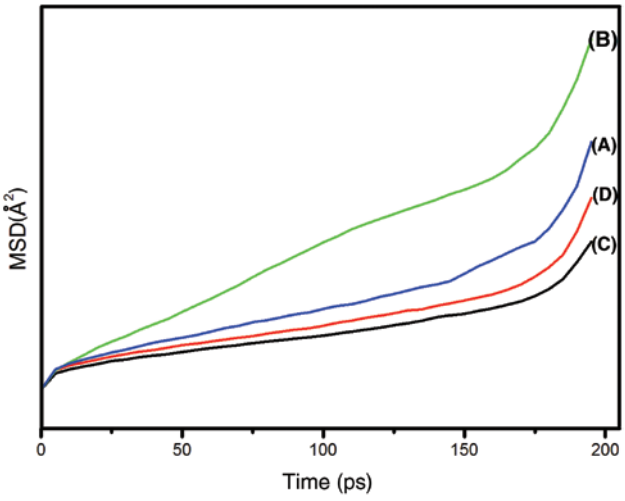

Figure 3: The MSD curves of the polymer chains: (A) membrane **3**, (B) membrane **4**, (C) membrane **5** and (D) membrane **6**.

mobility. The T_gs of membranes **4**, **5** and **6** were -10.776, 20.354 and 8.148°C, respectively, and the T_g of membrane **3** as recorded in (17) was 4.179°C. The chains mobility obtained from T_gs agreed well with the MSD results.

There are two phases in the polymer membrane: an occupied volume by polymer chains, and a free volume. The larger FFV reflects the higher amount and larger size of the voids in the polymer bulk, and contributes to the release of the drug molecules inside the polymers. The overall FFVs (the FFV probed by a probe with the radius 0.00 Å) of four different polymer membranes are listed in Table 3. The order of the FFV results is: membrane **4**>membrane **3**>membrane **6**>membrane **5**.

The simulation results of MSD and FFV shows the same tendency with the permeation rates of drug molecules transporting through the polymer membranes. By comparing the structures of the third monomer, we can acquire the following structure-performance relationship: the polymer chains' mobility decreases, and permeation rate correspondingly decreases with the increase in the amount of side groups, such as membranes **3** and **4**; the fractional free volume of the polymer chains decreases, and permeation rate correspondingly decreases with the increase in the volume of the side group, such as membranes **3**, **5** and **6**.

3 Conclusions

As an important component in the TDDs, the rate-controlling membrane makes sure drug delivery is at a sustained rate. How to design and synthesize membranes with satisfied rate-controlling properties is an attractive project. Here the relationship between polymers' structure and their release behaviors is investigated by molecular dynamics simulation. The simulation result shows a lesser amount and smaller volume of side groups on the double bonds in the monomer units, results in higher chain mobility and larger fractional free volume of the polymer membranes, and corresponding higher permeation rates. Moreover, these membranes are non-toxic by cytotoxicity evaluation. We can predict that the polyacrylates materials will be used in many fields including TDDs, filtration and separation and biomedicine delivery in the future, owing to its tailoring permeability and low cytotoxicity.

Table 3: The fractional free volume of four membranes.

Membrane	FFV (%)
3	28.59
4	29.26
5	26.26
6	27.51

4 Experimental part

4.1 Materials

2-Hydroxy-3-phenoxypropyl acrylate, 4-hydroxybutyl acrylate, 2-butoxyethyl acrylate, 2-phenoxyethyl methacrylate and isodecyl methacrylate (Sigma-Aldrich Corporation, WI, USA) were purified by vacuum distillation under reduced pressure and stored at 4°C for further use. Benzoyl peroxide and clonidine HCl (National Medicine Corporation, Shanghai, China) were used as received.

The L929 murine fibroblast cell was purchased from the Type Culture Collection of the Chinese Academy of Science (Shanghai, China). High glucose DMEM, fetal bovine serum (FBS), penicillin/streptomycin, trypsin and phosphate-buffered saline (PBS) were purchased from Thermo-Fisher HyClone (Logan, UT, USA). 3-(4,5-Dimethylthiazol-2-yl)-2,5-diphenyltetrazoliumbromide (MTT) was purchased from Aladdin (Shanghai, China).

All the other chemicals (National Medicine Corporation, Shanghai, China) received were of the highest purity and used without further purification.

4.2 Synthesis of the polyacrylates membranes

The synthesis of the polyacrylates membranes was as previously published (17), in brief, three monomers with 3% (w/w) benzoyl peroxide were dissolved completely and then were treated under the UV light (wavelength: 200–400 nm; power: 3 kW) for about 5 min. Three monomers in membrane **4** were 2-hydroxy-3-phenoxypropyl acrylate, 4-hydroxybutyl acrylate and 2-butoxyethyl acrylate with the weight ratio of 4:4:2. Three monomers in membrane **5** were 2-hydroxy-3-phenoxypropyl acrylate, 4-hydroxybutyl acrylate and 2-phenoxy ethyl methacrylate with the weight ratio of 4:4:2. Three monomers in membrane **6** were 2-hydroxy-3-phenoxypropyl acrylate, 4-hydroxybutyl acrylate and isodecyl methacrylate with the weight ratio of 4:4:2.

4.3 Characterization of the polyacrylates membranes

FTIR spectra of the thin freeze-dry membranes were recorded on a Nicolet iS10 FT-IR spectrometer (Thermo

Fisher Scientific, Waltham, MA USA) at a resolution of 4 cm^{-1} with 16 times of scanning over a wavenumber range of 450–4000 cm^{-1}.

The values of the glass transition temperature (T_g) of the membranes were collected on a DSC 204F1 differential scanning calorimeter (Netzsch, Selb, Germany). The samples weighing approximately 5 mg were first heated from 20°C to 200°C at a heating rate of 10°C/min and then held for 5 min to eliminate the thermal history. Subsequently, the samples were cooled to -60°C under a N_2 atmosphere and then heated again from -60°C to 200°C at a rate of 10°C/min.

The film thickness of dried membranes was measured using a digital meter (Shanghai Measuring and Cutting Tools Factory, Shanghai, China) with 0.001 mm accuracy. Five measurements were taken for each sample.

4.4 *In vitro* cytotoxicity studies

The L929 cell with high sensitivity to toxin, was selected for study of cytotoxicity (34). L929 cells were cultured in DMEM supplied with 10% FBS, 1% penicillin/streptomycin and incubated at a standard culture condition (37°C, 5% CO_2 in air) (Thermo Fisher Scientific, Waltham, MA, USA). The culture medium was refreshed every 2 days.

The cytotoxic effects of the membranes were evaluated by an indirect cytotoxicity test using the MTT assay (35). The cytotoxicity tests of samples were done according to ISO 10993-5 (Third Edition, 2009). L929 cells were seeded into 96-well plates at a seeding density of 5000 cells/well and incubated overnight. The sample was cut to 30 mg per disk, and then two sides of the sample were sterilized with UV for 24 h, respectively. Each sample was incubated in 5 ml DMEM medium for 5 days at 37°C, followed by filtration and mixing with 10% (v/v) FBS. One hundred micro liters of the sample extra was transferred into each well. The blank control groups were prepared by the same procedure without sample treatment. Five replicates of each sample were performed in each plate. After 1, 2 and 3 days treatment, respectively, the treatment medium was removed, 150 µl of cultur medium and 20 µl of MTT solution (5 mg/ml in PBS) were added to each well. After 4 h incubation the medium was discarded, 150 µl of DMSO was added to each well, and then the plate was shaken for 10 min to dissolve the formazan crystals. The optical density (OD) was measured at 492 nm with a reference wavelength 630 nm using a Multiskan MK3 microplate reader (Thermo Fisher Scientific, Waltham, MA, USA). All samples were repeated three times to ensure reproducibility.

The relative growth ratio (RGR) was calculated using the following equation, and the cytotoxicity was evaluated according to Table 4. The lower the RGR% value, the higher the cytotoxic potential of the test sample. According to ISO 10993-5:2009, if RGR% is reduced to <75% of the blank, it has a cytotoxic potential.

$$\mathrm{RGR}(\%)=\frac{\mathrm{OD}_{490(\mathrm{sample})}-\mathrm{OD}_{630(\mathrm{sample})}}{\mathrm{OD}_{490(\mathrm{blank})}-\mathrm{OD}_{630(\mathrm{blank})}}\times 100$$

4.5 *In vitro* release study

The release of the drug from the membrane was carried out using a modified Franz cell with 0.785 cm^2 of diffusion area and a receptor chamber of 9 ml volume. The prepared membrane was used as the diffusion membrane. An aqueous solution of 3.0 mg/ml clonidine HCl was used as the tested drug. PBS (pH 7.4) was used as a diffusion medium in the receptor chamber, stirred at 200 rpm at 37°C. At predetermined time intervals, 200 µl solution in the receptor chamber was withdrawn and then replaced an equal volume of fresh PBS. The samples withdrawn were analyzed for clonidine content by HPLC. Each test was carried out in triplicate (36).

The cumulative amount of clonidine HCl was calculated as follows:

$$Q=\frac{C_nV+\sum_{i=1}^{i=n-1}C_iV_i}{A}$$

where Q is the cumulative amount of the drug (µg/cm^2), V is the volume of receptor solution (ml), V_i is the volume of sample withdrawn (ml), C_n and C_i are the drug concentrations of the receptor solution and of the sample withdrawn (µg/ml), respectively, and A is the diffusion area (cm^2).

When the cumulative drug amount (Q_t, µg/cm^2) was plotted vs. time (T, h), the slope of the linear portion of the

Table 4: Cytotoxicity grades as a function of RGR.

Grade	0	1	2	3	4	5
RGR	≥100%	75%~99%	50%~74%	25%~49%	1%~24%	0%
Cytotoxicity	None	Slight	Mild	Moderate	Severe	Severe

plot was presented as the permeation rate [J, μg/(cm^2·h)]. The intercept on the x-axis was presented as the lag time (T_L, h).

4.6 HPLC analysis of clonidine HCl

The HPLC system (Waters, Milford, USA) consisted of a 1525 binary pump, a 717 plus auto-sampler and a 2487 dual-wavelength UV absorbance detector. Data acquisition and processing were dealt with by Waters Empower professional software. The mobile phase was a mixture of a buffer solution (1.16 g of d-10-camphorsulfonic acid dissolved in 1000 ml of 0.1 M sodium acetate): acetonitrile: methanol in the volume ratio of 6:1:1, and then adjusted to pH 3.0 with phosphate acid. The mobile phase was filtered through a 0.45 μm porosity filter and degassed. The liquid chromatograph was equipped with a 5 μm, 4.6 mm×150 mm C8 column (Agilent Eclipse XDB) with a flow rate of 1 ml/min. The volume of each injected sample was 20 μl, the wavelength of the UV detector was set at 220 nm, and the run time was 10 min (36).

4.7 Molecular dynamics simulation

As a computer simulation method, molecular dynamics (MD) simulation can calculate the physical movements of atoms and molecules properties of the membrane at the molecular level (37, 38). Polymer chain mobility was analyzed by mean-square displacement (MSD) and free volume characteristics of membrane were investigated by a Connolly surface.

MD simulations were carried out using "Amorphous cell", "Discover" and "Forcite" modules of Materials Studio 7.0 (Accelrys Software Inc., San Diego, USA). The energy minimization process was conducted using the smart minimizer method. Non-bond cutoff distance was defined as 12.5 Å (with a spline width of 1.0 Å and a buffer width of 0.5 Å).

First, an amorphous cell containing a polymer chain consisting of 100 repeat unit was built. Then, geometry optimization was performed by setting a maximum number of iterations to 50,000 or convergence tolerance energy to 0.001 kcal/mol. And then, a 200 ps dynamics equilibration process on the system was run with 1 fs time step in the NVT (T=298 K) ensemble to obtain the equilibrium molecular structures and the atomic trajectory was recorded for the analysis of mean square displacement (MSD) of the polymer chain.

To estimate free volume inside each polymer membrane, fractional free volume (FFV) was calculated as follows (38, 39):

$$\mathrm{FFV} = \frac{V_{\mathrm{free}}}{V_{\mathrm{free}} + V_{\mathrm{occupy}}}$$

where V_{free} and V_{occupy} are the free volume and occupied volume.

Acknowledgments: This work was supported by the National Significant and Special Project of New Created Drugs (No. 2010ZX09401-404).

References

1. Denkbas EB, Ottenbrite RM. Perspectives on: chitosan drug delivery systems based on their geometries. J Bioact Compat Pol. 2006;21(4):351–8.
2. Vaghani SS, Patel MM, Satish CS, Patel KM, Jivani NP. Synthesis and characterization of carboxymethyl chitosan hydrogel: application as pH-sensitive delivery for nateglinide. Curr Drug Deliv. 2012;9(6):628–6.
3. Wang W, Zhang P, Shan W, Gao J, Liang W. A novel chitosan-based thermosensitive hydrogel containing doxorubicin liposomes for topical cancer therapy. J Biomat Sci Polym E. 2013;24(14):1649–59.
4. Ngoc-Thang N, Liu J. Fabrication and characterization of poly(vinyl alcohol)/chitosan hydrogel thin films via UV irradiation. Eur Polym J. 2013;49(12):4201–11.
5. Pawar SN, Edgar KJ. Alginate derivatization: a review of chemistry, properties and applications. Biomaterials 2012;33(11):3279–305.
6. Chen DW, Hsu Y, Liao J, Liu S, Chen J, Ueng SW. Sustainable release of vancomycin, gentamicin and lidocaine from novel electrospun sandwich-structured PLGA/collagen nanofibrous membranes. Int J Pharm. 2012;430(1–2):335–41.
7. Parizek M, Douglas TE, Novotna K, Kromka A, Brady MA, Renzing A, Voss E, Jarosova M, Palatinus L, Tesarek P, Ryparova P, Lisa V, Santos AM, Bacakova L. Nanofibrous poly(lactide-co-glycolide) membranes loaded with diamond nanoparticles as promising substrates for bone tissue engineering. Int J Nanomed. 2012;7:1931–51.
8. Xu Q, Huang W, Jiang L, Lei Z, Li X, Deng H. KGM and PMAA based pH-sensitive interpenetrating polymer network hydrogel for controlled drug release. Carbohyd Polym. 2013;97(2):565–70.
9. Tirnaksiz F, Yuce Z. Development of transdermal system containing nicotine by using sustained release dosage design. Farmaco 2005;60(9):763–70.
10. Fang JY, Huang YB, Wang HY, Tsai YH. Electrically-assisted skin permeation of two synthetic capsaicin derivatives, sodium nonivamide acetate and sodium nonivamide propionate, via rate-controlling polyethylenemembranes. Biol Pharm Bull. 2005;28(9):1695–1701.

11. Tang M, Hou J, Lei L, Liu X, Guo S, Wang Z, Chen K. Preparation, characterization and properties of partially hydrolyzed ethylene vinyl acetatecopolymer films for controlled drug release. Int J Pharm. 2010;400(1–2):6–73.
12. Kim MK, Zhao H, Lee CH, Kim DD. Formulation of a reservoir-type testosterone transdermal delivery system. Int J Pharm. 2001;219(1–2):51–9.
13. Babu RJ, Pandit JK. Effect of penetration enhancers on the release and skin permeation of bupranolol from reservoir-type transdermal delivery systems. Int J Pharm. 2005;288(2):325–34.
14. El-Newehy MH, Al-Deyab SS, Kenawy ER, Abdel-Megeed A. Nanospider technology for the production of nylon-6 nanofibers for biomedical applications. J Nanomater. 2011, Article ID 626589.
15. Suksaeree J, Pichayakorn W, Monton C, Sakunpak A, Chusut T, Saingam W. Rubber polymers for transdermal drug delivery systems. Ind Eng Chem Res. 2014;53(2):507–13.
16. Pichayakorn W, Suksaeree J, Boonme P, Taweepreda W, Amnuaikit T, Ritthidej GC. Deproteinised natural rubber used as a controlling layer membrane in reservoir-type nicotine transdermal patches. Chem Eng Res Des. 2013;91(3):520–9.
17. Zhan X, Chen S, Tang G, Mao Z. Two new types of copolymer membranes controlling clonidine zero-order release. J Appl Polym Sci. 2007;106(5):3016–22.
18. Zhan X, Mao Z, Chen J, Zhang Y. Acrylate copolymer: a rate-controlling membrane in the transdermal drug delivery system. e-Polymers 2015;15(1):55–63.
19. Schmidt LE, Leterrier Y, Vesin J, Wilhelm M, Månson JE. Photorheology of fast UV-curing multifunctional acrylates. Macromol Mater Eng. 2005;290(11):1115–24.
20. Fiume MZ. Final report on the safety assessment of acrylates copolymer and 33 related cosmetic ingredients. Int J Toxicol. 2002;21(6 Suppl. 3):1–50.
21. Kilambi H, Konopka D, Stansbury JW, Bowman CN. Factors affecting the sensitivity to acid inhibition in novel acrylates characterized by secondary functionalities. J Polym Sci Pol Chem. 2007;45(7):1287–95.
22. Brahim S, Narinesingh D, Elie AG. Synthesis and hydration properties of pH-sensitive p(HEMA)-based hydrogels containing 3-(trimethoxysilyl)propyl methacrylate. Biomacromolecules 2003;4(3):497–503.
23. Lahooti S, Sefton MV. Microencapsulation of normal and transfected L929 fibroblasts in a HEMA-MMA copolymer. Tissue Eng. 2000;6(2):139–49.
24. Babić MM, Jovašević JS, Filipović JM, Tomić SL. Diffusion of drugs in hydrogels based on (meth)acrylates, poly(alkylene glycol) (meth)acrylates and itaconic acid. Hem Ind. 2012;66(6):823–9.
25. Zhan X, Chen S, Tang G, Mao Z. Poly(2-hydroxy-3-phenoxypropylacrylate, 4-hydroxybutyl acrylate, dibutyl maleate) membrane controlled clonidine zero-order release. Eur J Pharm Biopharm. 2007;66(3):429–34.
26. Zhan X, Chen S, Tang G, Mao Z. A new poly(2-hydroxy-3-phenoxypropylacrylate, 4-hydroxybutyl acrylate, diethyl maleate) membrane controlled clonidine linear release in the transdermal drug delivery system. Eur Polym J. 2007;43(4):1588–94.
27. Choi K, Jo WH. Effect of chain flexibility on selectivity in the gas separation process: Molecular dynamics simulation. Macromolecules 1995;28(25):8598–603.
28. Tung KL, Lu KT. Effect of tacticity of PMMA on gas transport through membranes: MD and MC simulation studies. J Membrane Sci. 2006;272(1–2):37–49.
29. Yoshinori T, Hideki T, Koichiro N. Molecular simulation of permeation of small penetrants through membranes. 1. Diffusion coefficients. Macromolecules 1994;27(16):4498–508.
30. Karayiannis NC, Mavrantzas VG, Theodorou DN. Detailed atomistic simulation of the segmental dynamics and barrier properties of amorphous poly(ethylene terephthalate) and poly(ethylene isophthalate). Macromolecules 2004;37(8):2978–95.
31. Nagel C, Schmidtke E, Günther-Schade K, Hofmann D, Fritsch D, Strunskus T, Faupel F. Free volume distributions in glassy polymer membranes: comparison between molecular modeling and experiments. Macromolecules 2000;33(6):2242–8.
32. Oprea S, Oprea V. Synthesis and characterization of the cross-linked polyurethane–gum arabic blends obtained by multiacrylates cross-linking polymerization. J Elastom Plast. 2012;45(6):564–76.
33. Park J, Lee Y, Park H, Kim H. Preparation and properties of UV-curable fluorinated polyurethane acrylates. J Appl Polym Sci. 2014;131(16), Doi: 10.1002/APP.40603.
34. Wu JC, Ray S, Gizdavic-Nikolaidis M, Uy B, Swift S, Jin J, Cooney RP. Nanostructured bioactive material based on polycaprolactone and polyaniline fiber-scaffolds. Synthetic Met. 2014;198:41–50.
35. Kong N, Jiang T, Zhou Z, Fu J. Cytotoxicity of polymerized resin cements on human dental pulp cells in vitro. Dent Mater. 2009;25(11):1371–5.
36. Zhan X, Tang G, Chen S, Mao Z. A new copolymer membrane controlling clonidine linear release in a transdermal drug delivery system. Int J Pharm. 2006;322(1–2):1–5.
37. Ling C, Liang X, Fan F, Yang Z. Diffusion behavior of the model diesel components in different polymer membranes by molecular dynamic simulation. Chem Eng Sci. 2012;84:292–302.
38. Pan F, Peng F, Jiang Z. Diffusion behavior of benzene/cyclohexane molecules in poly(vinyl alcohol)-graphite hybrid membranes by molecular dynamics simulation. Chem Eng Sci. 2007;62:703–10.
39. Bondi A. Van der Waals volumes and radii. J Phys Chem. 1964;68(3):441–51.